

Magnetic Nanoparticle Supported Ionic Liquid Phase Catalyst for Oxidation of Alcohols

Altafhusen Naikwade,^A Megha Jagadale,^A Dolly Kale,^A and
Gajanan Rashinkar ^{A,B}

^ADepartment of Chemistry, Shivaji University, Kolhapur, 416004, Maharashtra, India.

^BCorresponding author. Email: gsr_chem@unishivaji.ac.in

A new magnetic nanoparticle supported ionic liquid phase (SILP) catalyst containing perruthenate anions was prepared by a multistep procedure. The various analytical techniques such as FT-IR spectroscopy, X-ray photoelectron spectroscopy, transmission electron microscopy, thermogravimetric analysis, energy dispersive X-ray analysis, and vibrating sample magnetometer analysis ascertained the successful formation of catalyst. The performance of a magnetically retrievable SILP catalyst was evaluated in the selective oxidation of alcohols. The split test and leaching studies of the SILP catalyst confirmed its heterogeneous nature. In addition, the reusability potential of SILP catalyst was also investigated which revealed its robust activity up to six consecutive cycles.

Manuscript received: 4 December 2019.

Manuscript accepted: 26 February 2020.

Published online: 25 June 2020.

Introduction

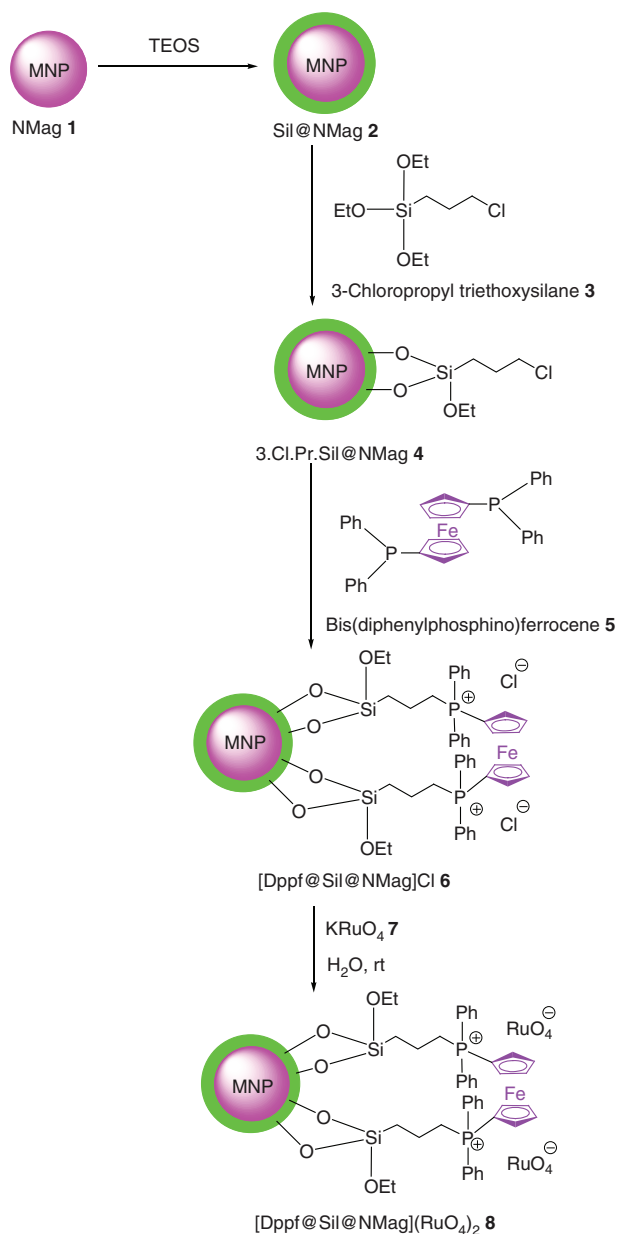
The redesigning of chemical processes to avoid generation of toxic waste and utilisation of hazardous substances has attracted a great deal of attention, as green chemistry is becoming a pivotal issue.^[1,2] In this context, supported ionic liquid phase (SILP) catalysis has originated as a subject of interest among the scientific community. The concept of SILP catalysis involves immobilization of ionic liquid (IL)-mimicking units onto a high surface area support material.^[3–6] The various drawbacks associated with ILs could be circumvented by employing these advanced materials in catalysis as powerful green tools. The interest in SILP catalysts emanate from their fascinating properties such as ease of product separation, selectivity, high catalytic activity, efficient reusability, and ecologically benign nature. Moreover, SILP catalysis may facilitate the application of fixed bed reactors for chemical transformations in continuous mode.^[7] SILP catalysis has achieved tremendous advances over the past few years providing facile access to a large number of privileged scaffolds under environmentally benign conditions.

Magnetic nanoparticles (MNPs) have been widely exploited in various domains. The application of MNPs in the catalysis arena has been a subject of intense research. MNPs have recently emerged as a viable alternative to conventional catalytic supports for the design of heterogeneous catalytic systems. The magnetically retrievable nano-catalytic systems have been explored for their potential in addressing various environmental and economic issues.^[8] Surface functionalized MNPs are an elegant pathway to bridge the gap between heterogeneous and homogeneous catalysis.^[9] Amongst several MNPs, Fe₃O₄ MNPs have attractive properties like low toxicity, unique magnetic properties, high surface area, good dispersivity, and magnetic retrievability.^[10] These properties are of use for a myriad of applications in magnetically retrievable catalysis,^[11–16] bioseparation,^[17] biomedical and bioengineering,^[18,19] environmental treatment,^[20]

and food analysis.^[21] The applicability of Fe₃O₄ MNP-based SILP nanocatalysts have witnessed an enormous growth to organic transformations due to continuous increasing emphasis on developing greener pathways.^[22–30] However, despite the substantial progress, there is still room for development especially towards designing green procedures using magnetically retrievable supported ionic liquid-like phase catalysts.

The selective oxidation of primary alcohols to aldehydes has been a reaction of immense importance in synthetic chemistry. Aldehydes are considered as privileged motifs due to their extensive applications such as intermediates in the manufacturing of agrochemicals, dyes, pharmaceuticals, and fine chemicals particularly for the perfume industry.^[31,32] Consequently, a plethora of synthetic strategies for the oxidation of alcohols have been unceasingly reported employing catalytic systems with perruthenate anions.^[33–38] Efforts have also been devoted to using different oxidants,^[39–43] transition metals,^[44–52] and SILP catalysts.^[53–55] However, despite the impressive progress, various challenges still exist that are associated with difficulty in the separation and disposal of expensive or toxic stoichiometric reagents. Moreover, the utilisation of excess catalysts leads to generation of significant amounts of unwanted by-products affording poor atom economy and high E-factors. The cautious handling of sensitive reagents and removal of unwanted by-products has become a tedious task.^[56,57] Consequently, there is an urgent need to design robust heterogeneous catalytic systems especially for oxidation of primary alcohols.

In continuance of our prior work regarding green chemistry,^[58–60] we disclose herein a new approach for the preparation of a Fe₃O₄ MNP SILP catalyst containing perruthenate anions and evaluated its potential as a heterogeneous catalyst for the oxidation of primary alcohols.



Scheme 1. Preparation of $[\text{Dppf}@Sil@NMag](\text{RuO}_4)_2$ **8**.

Results and Discussion

The preparative route for the MNP SILP catalyst containing perruthenate anions is shown in **Scheme 1**. First, a chemical coprecipitation approach was used to prepare Fe_3O_4 MNPs (NMag, **1**). The surface of **1** was then coated by a sol-gel approach with a silica shell to furnish Sil@NMag **2**. The organofunctionalization of **2** was achieved with 3-chloropropyltriethoxysilane **3** to yield Fe_3O_4 MNPs with a chlorofunctionalized surface abbreviated as 3.Cl.Pr.Sil@NMag **4**. The unique ability of surface active silanol moieties of **2** facilitates the generation of strong siloxane bonds (Si–O–Si) with the silyl ether group of **3**. The IL-mimic unit was then grafted on **4** by reacting with bis(diphenylphosphino)ferrocene **5** to furnish the precursor abbreviated as $[\text{Dppf}@Sil@NMag]\text{Cl}$ **6**. Lastly, **6** underwent an anion metathesis reaction with KRuO_4 **7** to afford the desired Fe_3O_4 MNP SILP catalyst containing perruthenate anions, namely $[\text{Dppf}@Sil@NMag](\text{RuO}_4)_2$ **8**.

The surface modifications of the Fe_3O_4 nanocore during the preparation of $[\text{Dppf}@Sil@NMag](\text{RuO}_4)_2$ **8** were monitored

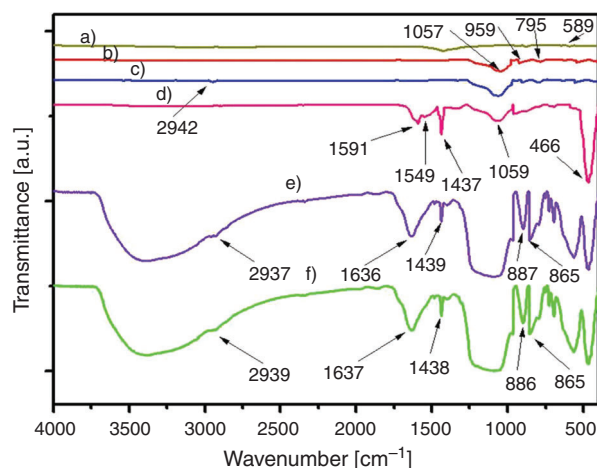


Fig. 1. FT-IR spectra of (a) NMag **1**, (b) Sil@NMag **2**, (c) 3.Cl.Pr.Sil@NMag **4**, (d) $[\text{Dppf}@Sil@NMag]\text{Cl}$ **6**, (e) $[\text{Dppf}@Sil@NMag](\text{RuO}_4)_2$ **8** before reaction, and (f) $[\text{Dppf}@Sil@NMag](\text{RuO}_4)_2$ **8** after six consecutive runs.

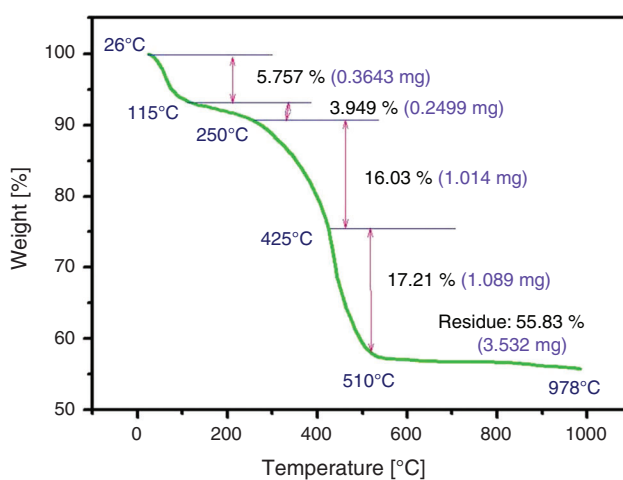


Fig. 2. TGA curve of $[\text{Dppf}@Sil@NMag](\text{RuO}_4)_2$ **8**.

by FT-IR spectroscopy. In the FT-IR spectrum of NMag **1**, a characteristic band appeared at 589 cm^{-1} and was assigned to Fe–O stretching vibrations of the Fe_3O_4 MNPs. The coating of a silica shell on **1** was evidenced by FT-IR peaks at 959 cm^{-1} (Si–O) symmetric, 1057 cm^{-1} (Si–O–Si) siloxane asymmetric, and 795 cm^{-1} (Si–O–Si) siloxane symmetric stretching modes (**Fig. 1a**).^[61] The FT-IR spectrum of 3.Cl.Pr.Sil@NMag **4** showed a distinct peak for the stretching vibration of C–H of the propyl group at 2942 cm^{-1} (**Fig. 1b**).^[62] The covalent grafting of bis(diphenylphosphino)ferrocene **5** onto **4** was evident from the FT-IR spectrum of $[\text{Dppf}@Sil@NMag]\text{Cl}$ **6**, which displayed bands in the region $1600\text{--}1450\text{ cm}^{-1}$ for the C=C stretching of the aromatic ring, and 1437 and 466 cm^{-1} for P–CH₂ and Fe–Cp stretching, respectively (**Fig. 1c**).^[63] In the FT-IR spectrum of **8** (**Fig. 1d**), the characteristic peaks observed at 887 and 865 cm^{-1} are attributed to symmetric and asymmetric stretching vibrations of Ru=O. The presence of these peaks strongly suggest the successful immobilization of perruthenate anions on **8**.^[64]

The quantification of the perruthenate anion content in $[\text{Dppf}@Sil@NMag](\text{RuO}_4)_2$ **8** was carried out by energy-dispersive X-ray (EDX) spectroscopy. The EDX elemental mapping revealed the presence of 0.11 mmol of perruthenate anion per gram of **8**.

The thermogravimetric analysis (TGA) of $[\text{Dppf}@Sil@NMag](\text{RuO}_4)_2$ **8** is depicted in **Fig. 2**. The thermal profile of **8** displayed

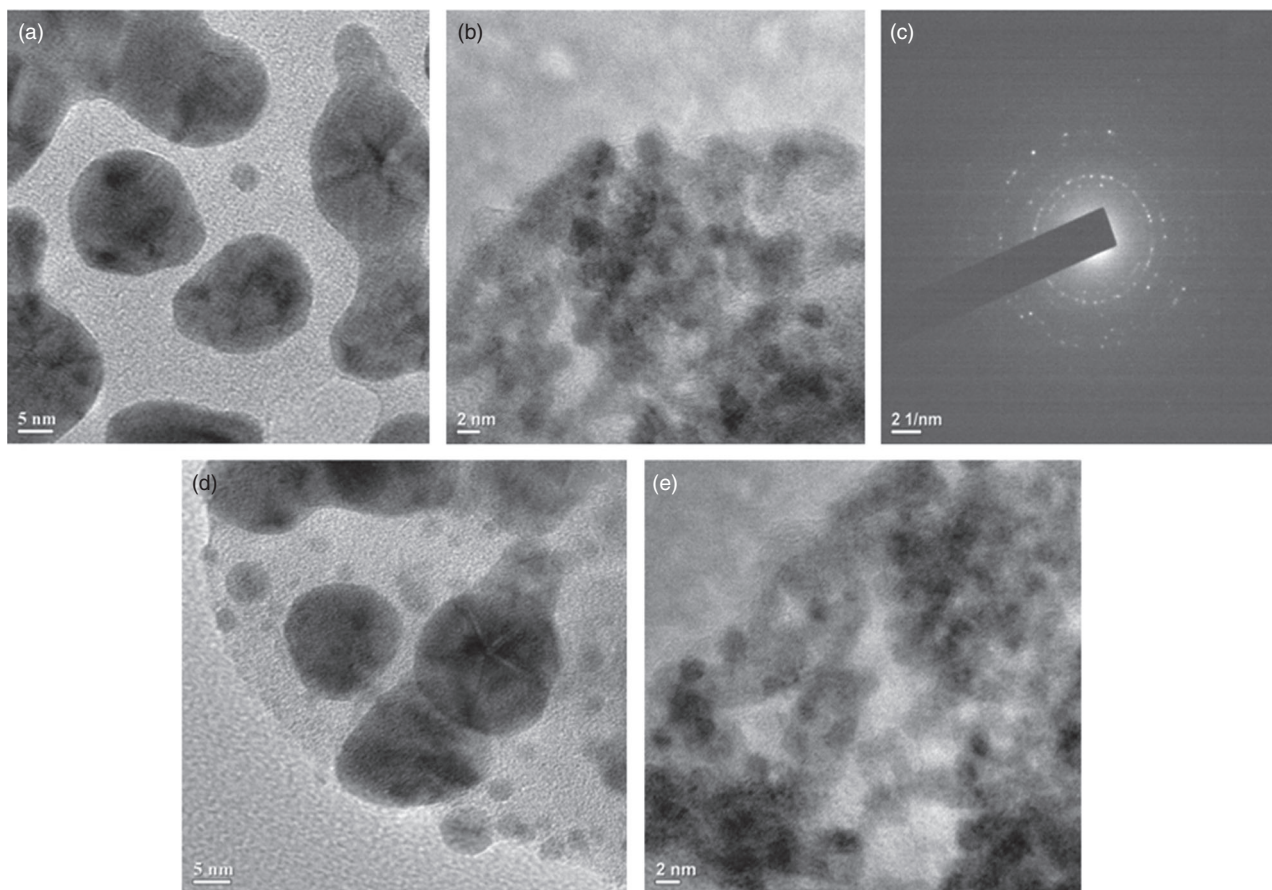


Fig. 3. TEM images of [Dppf@Sil@NMag](RuO₄)₂ **8** with SAED pattern (a–c) before reaction and [Dppf@Sil@NMag](RuO₄)₂ **8** after sixth run (d–e).

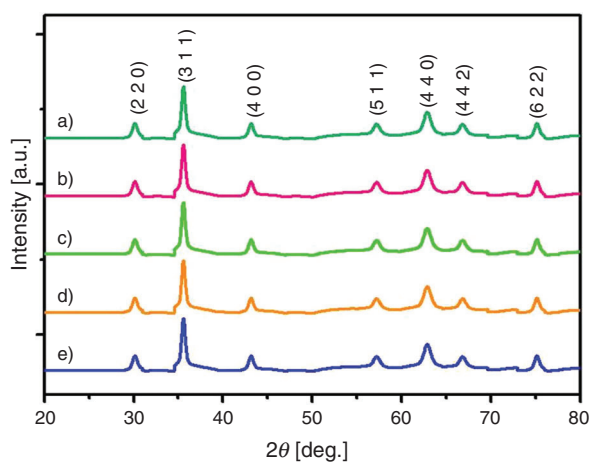


Fig. 4. XRD pattern of (a) Sil@NMag **2**, (b) 3.Cl.Pr.Sil@NMag **4**, (c) [Dppf@Sil@NMag]Cl **6**, (d) [Dppf@Sil@NMag](RuO₄)₂ **8** before reaction, and (e) [Dppf@Sil@NMag](RuO₄)₂ **8** after six consecutive runs.

an initial weight loss of 5.75% due to evaporation of physisorbed water at 115°C. Furthermore, a minor mass loss of 3.94% centred around 250°C followed by two major mass losses of 16.03 and 17.21% at 425 and 510°C are observed by related thermal collapse of organic layers on the surface of core–shell MNPs and the perruthenate anion. Lastly, the generation of thermostable metallic oxides and silica contributes large residual weight.

The transmission electron microscopy (TEM) images of [Dppf@Sil@NMag](RuO₄)₂ **8** before and after catalysis (after sixth run) are shown in Fig. 3a–d. TEM images showed the quasispherical particles with a core–shell structure.^[30] Fe₃O₄ MNPs have an average diameter of 2–11 nm. The selected area electron diffraction (SAED) pattern demonstrates the white dots and bright diffraction rings which designates the crystallinity of the Fe₃O₄ nanocore (Fig. 3c). Gratifyingly, qualitative alteration in morphologies of fresh and reused catalysts was not observed even after six consecutive runs.

The X-ray diffraction (XRD) patterns of Sil@NMag **2**, 3.Cl.Pr.Sil@NMag **4**, [Dppf@Sil@NMag]Cl **6**, and [Dppf@Sil@NMag](RuO₄)₂ **8** before and after catalysis (after sixth run) are depicted in Fig. 4a–e. The diffraction peaks were well coordinated to the cubic inverse spinel structure of Fe₃O₄ and are consistent with JCPDS card no. 86-1339. All five materials display characteristic diffraction peaks at 2θ values of 30.17°, 35.49°, 43.12°, 57.12°, 62.64°, 66.83°, and 75.09° being assigned to the (2 2 0), (3 1 1), (4 0 0), (5 1 1), (4 4 0), (4 4 2), and (6 2 2) crystal indices of a Fe₃O₄ cubic lattice respectively. The nearly identical reflections were displayed by all the materials, which revealed the behaviour of the Fe₃O₄ nanocore in a very stable mode.

X-Ray photoelectron spectroscopy (XPS) was employed to elucidate structural features of [Dppf@Sil@NMag](RuO₄)₂ **8**. The presence of Ru, O, C, Fe, Si, and P elements in **8** was confirmed by a survey spectrum obtained from XPS results (Fig. 5a). In the Fe 2p region the shift of the photoelectron peak

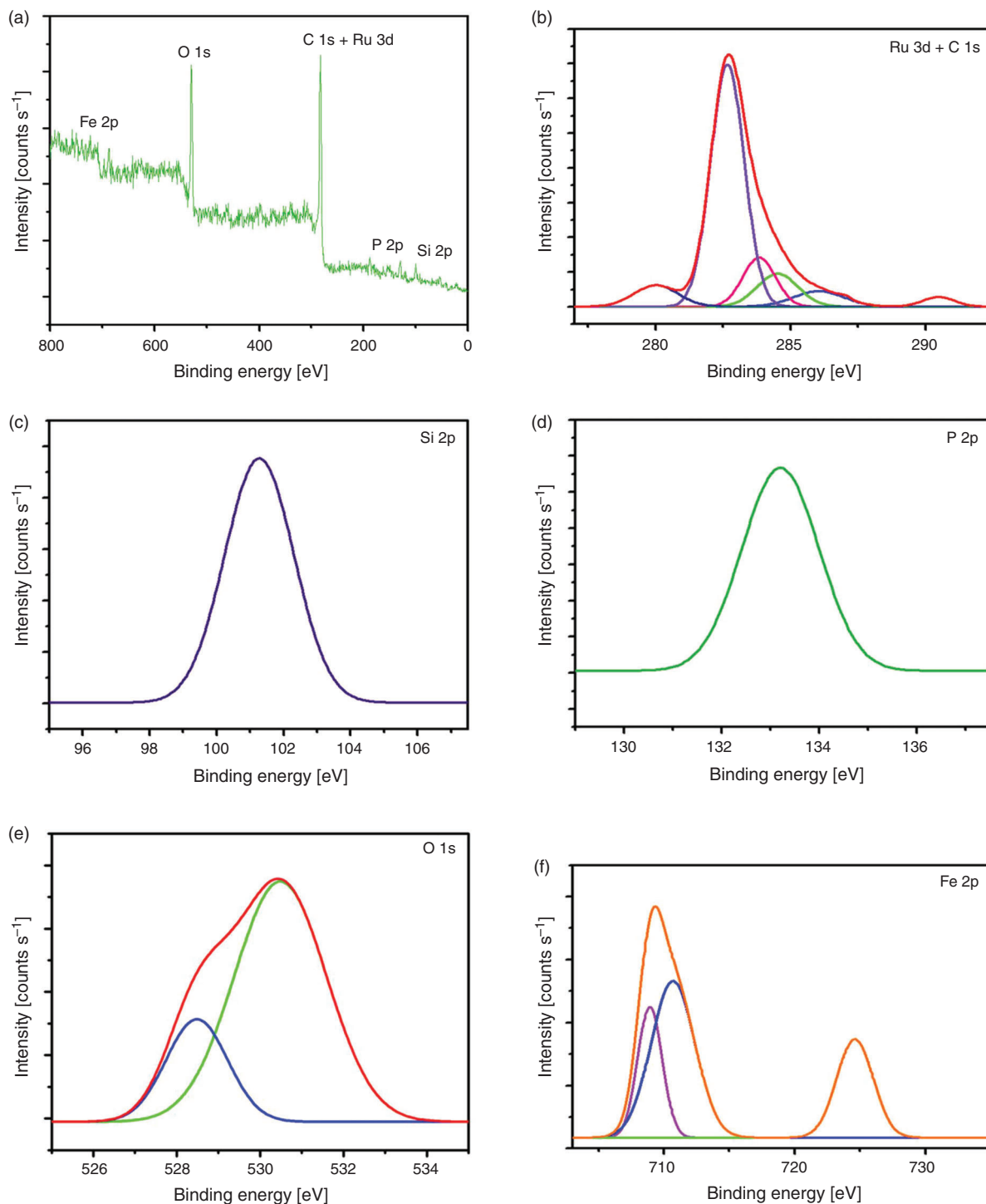


Fig. 5. XPS spectra of [Dppf@Sil@NMag](RuO₄)₂ (**8**): (a) survey spectrum, (b) Ru 3d and C 1s, (c) Si 2p, (d) P 2p, (e) O 1s, and (f) Fe 2p.

to higher binding energy is observed due to anchoring of ferrocene onto the material in comparison with free ferrocene. This fact was demonstrated by Dong and co-workers. In this work, the successful grafting of the ferrocene unit was confirmed by photoelectron peaks in the Fe 2p region positioned at 710.9 and 724.4 eV (Fig. 5f).^[65] The C 1s and Ru 3d core level spectrum splits into six photoelectron peaks centered at 280.0, 282.6, 283.9, 284.5, 285.9, and 290.5 eV (Fig. 5b). The photoelectron peak located at 282.6 eV corresponds to bonding between silicon and carbon. In addition, in the Si 2p

core level spectrum the signal at 101.2 eV also confirms the same fact (Fig. 5c).^[66] Moreover, the contribution of the perruthenate anion is designated by Ru 3d peaks at 280.0 (3d_{5/2}) and 283.9 eV (3d_{3/2}). The photoelectron peaks positioned at 290.5 and 284.5 eV are indicative of carbons of benzene rings and ferrocenyl carbons respectively.^[67,68] The presence of phosphonium cations (P⁺) bonded with sp³ hybridized carbons is corroborated by the photoelectron peak at 285.9 eV.^[69] The peak at 133.1 eV observed in the P 2p region also specifies the phosphonium ion (Fig. 5d).^[70] The peaks at 530.5 and

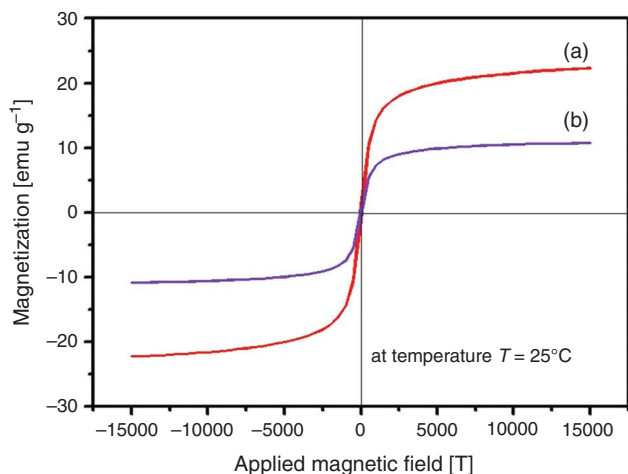


Fig. 6. Magnetization curves obtained by vibrating sample magnetometer analysis at room temperature: (a) bare MNPs and (b) [Dppf@Sil@NMag](RuO₄)₂ **8**.

Table 1. Optimization of catalyst loading in the [Dppf@Sil@NMag](RuO₄)₂ **8** promoted selective oxidation of benzyl alcohol

Entry ^A	Catalyst loading [mg (mol-%)]	Temperature [°C]	Time [h]	Yield ^B [%]
1	15 (0.17)	Rt	22	10
2	25 (0.29)	Rt	20	25
3	50 (0.59)	Rt	19	37
4	75 (0.89)	Rt	18	38
5	100 (1.18)	Rt	18	38
6	50 (0.59)	40	9	45
7	50 (0.59)	50	6	67
8	15 (0.17)	Reflux	10	37
9	25 (0.29)	Reflux	9	58
10	50 (0.59)	Reflux	2.5	97
11	75 (0.89)	Reflux	2.5	98
12	100 (1.18)	Reflux	2.5	98
13	No catalyst	Rt	24	None

^AReaction conditions: **9a** (1 mmol), THF (5 mL), and [Dppf@Sil@NMag](RuO₄)₂ **8**.

^BIsolated yield after column chromatography.

528.4 eV in the O 1s region are attributed to oxygen bonded with Si and lattice oxygen (Fig. 5e).^[71] Conclusively, the successful formation of **8** was confirmed by these structural features.

Vibrating sample magnetometry (VSM) was used to explore the magnetic behaviour of bare Fe₃O₄ MNPs **1** and [Dppf@Sil@NMag](RuO₄)₂ **8** at room temperature. The magnetic hysteresis curves in Fig. 6 illustrate lowering in the saturation magnetization (*M_s*) values from bare Fe₃O₄ MNPs (22 emu g⁻¹) to the final catalyst (11 emu g⁻¹). This decrease upon surface modification of the bare Fe₃O₄ MNPs **1** could be attributed to a shielding effect of the non-magnetic silica and organic moieties.^[72] In spite of this reduction in *M_s* values, **8** can be effortlessly isolated from the reaction medium with a permanent magnet.

Table 2. Screening of solvents for the [Dppf@Sil@NMag](RuO₄)₂ **8** promoted selective oxidation of benzyl alcohol

Entry ^A	Solvent	Time [h]	Yield ^B [%]
1	Toluene	17	69
2	Acetonitrile	19	68
3	1,4-Dioxane	16	70
4	Dichloromethane	24	44
5	THF	2.5	97
6	DMF	28	Trace
7	DMSO	24	Trace
8	Ethanol	21	41
9	Methanol	20	43

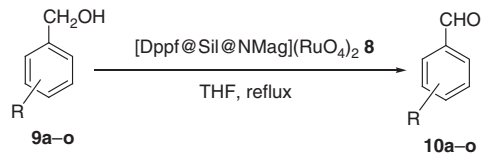
^AReaction conditions: **9a** (1 mmol), solvent (5 mL), and [Dppf@Sil@NMag](RuO₄)₂ **8** (50 mg).

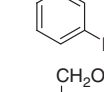
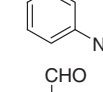
^BIsolated yield after column chromatography.

Afterwards, our efforts were directed to evaluate the catalytic potential of [Dppf@Sil@NMag](RuO₄)₂ **8** in the selective oxidation of primary alcohols. The optimization of reaction conditions was performed employing benzyl alcohol (**9a**) as a model substrate. The optimization of catalyst loading was our initial task. Different quantities of **8** were employed to perform a model reaction in THF at ambient temperature (Table 1, entries 1–5). The influence of temperature was found to be the crucial parameter. The reactions could not proceed to a synthetically useful degree at ambient temperature even after prolonged reaction time. An enhancement in the yield of product was observed with an increase in the reaction temperature (Table 1, entries 6–12). The increase in quantity of **8** from 15 to 50 mg was proven to be favourable, affording the corresponding product **10a** up to 97% yield (Table 1, entries 8–10). However, a rise in catalyst quantity (Table 1, entries 11–12) had no impact on yield of product. Therefore, 50 mg of catalyst under reflux reaction conditions was sufficient to drive the model reaction efficiently to furnish the anticipated product in excellent yield within 2.5 h (Table 1, entry 10). The reaction did not proceed even after an extended period in the absence of **8** (Table 1, entry 13) suggesting the crucial role of **8**.

Next, the model reaction was carried out for the screening array of solvents (Table 2). The solvents such as toluene, acetonitrile, and 1, 4-dioxane (Table 2, entries 1–3) furnished good yields. On the contrary, dichloromethane, methanol, and ethanol afforded lower yields of anticipated products (Table 2, entries 4, 8–9). The reaction progressed slowly in DMF and DMSO resulting in the formation of trace amounts of **10a** (Table 2, entries 6–7). THF was found to be the suitable choice for this protocol (Table 2, entry 5).

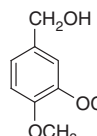
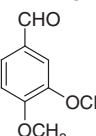
With the optimized reaction conditions, the substrate scope of the protocol was probed by performing oxidation of diversely substituted alcohols **9a–o** (Table 3). The electronic substitution in aromatic alcohols displayed a strong influence on the yield of reaction. Aromatic alcohols with electron-donating groups **9b–d**, **9j**, and **9o** afforded good yields (Table 3, entries 2–4, 10, and 15) as compared with that of aromatic alcohols bearing electron-withdrawing groups **9g**, **9h** and **9k** (Table 3, entries 7, 8, and 11). Gratifyingly, it is worth mentioning that heteroaromatic

Table 3. [Dppf@Sil@NMag](RuO₄)₂ **8** promoted selective oxidation of alcohols


Entry ^A	Alcohol	Product	Time [h]	Yield ^B [%]
1			2.5	97
2			3	89
3			4	92
4			3	96
5			3	85
6			4	89
7			5	88
8			4	89
9			5	86
10			5	84
11			4	92
12			4	89
13			5	86

(continued)

Table 3. (Continued)

Entry ^A	Alcohol	Product	Time [h]	Yield ^B [%]
14			4	92
15			4	87

^AReaction conditions: **9** (1 mmol), THF (5 mL), and [Dppf@Sil@NMag](RuO₄)₂ **8** (50 mg).^BIsolated yield after column chromatography.

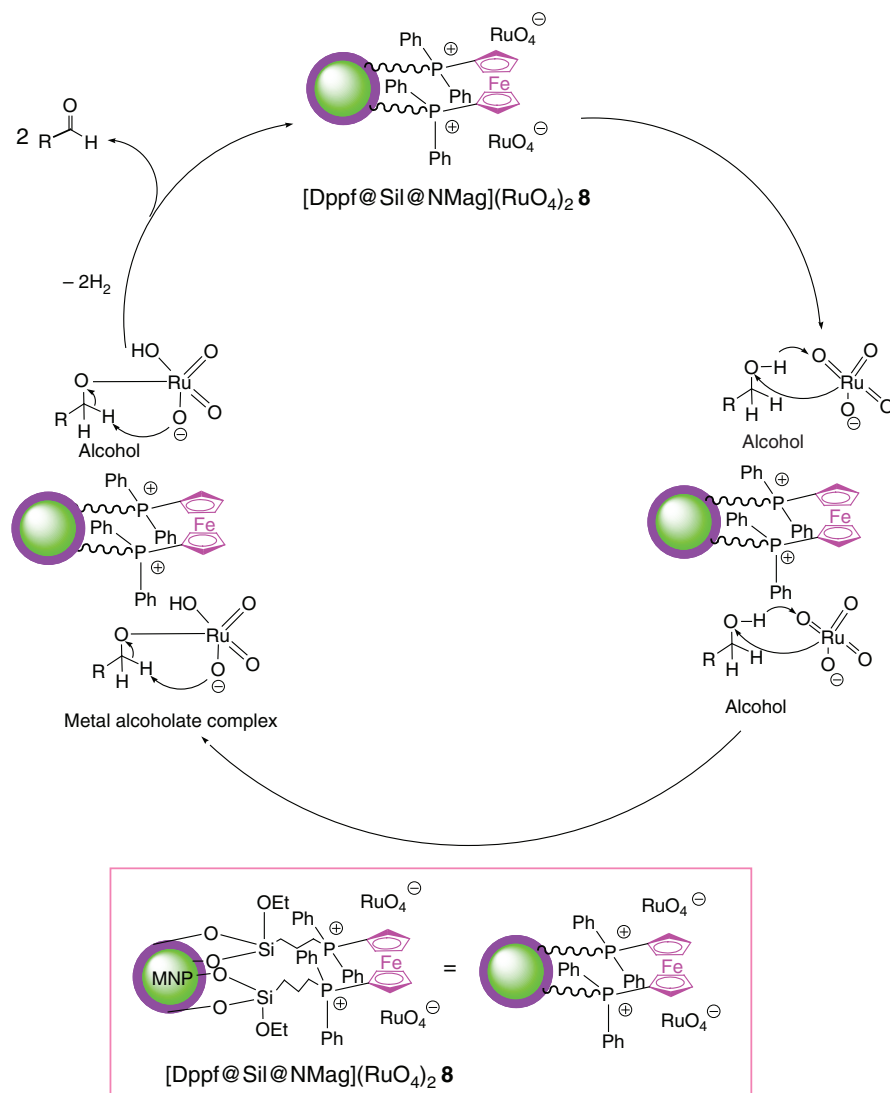
alcohols such as (pyridine-2-yl)methanol, (furan-2-yl)methanol, and (thiophen-2-yl)methanol (**9l–n**) showed the highest reactivity furnishing excellent yields of anticipated products (Table 3, entries 12–14). Despite steric congestion, sterically hindered alcohols such as *o*-methoxy, *o*-methyl, and *o*-nitro benzyl alcohols (**9c,f,i**) (Table 3, entries 3, 6 and 9) also afforded a good yield of corresponding products.

The formation of anticipated products was ascertained by spectroscopic techniques such as ¹H NMR, ¹³C NMR, and FT-IR spectroscopy and mass spectrometry (MS).

A plausible mechanism for the [Dppf@Sil@NMag](RuO₄)₂ **8** mediated oxidation of aromatic alcohols is depicted in Scheme 2. Initially, the alcohol attacks the perruthenate anion to afford a metal alcoholate complex following a free radical-like transition state.^[73–75] Subsequently, β-hydride elimination of the metal alcoholate complex with release of hydrogen leads to formation of corresponding aldehydes. The cation in **8** has profound influence on the performance of the catalyst. The presence of a bulky, cylindrical ferrocenyl moiety causes significant enhancement in the accessibility of reactants to the active site which has a strong influence on the catalytic performance of **8**.^[76–81] In addition, F₃O₄ nanocores assist the facile removal of the catalyst with a permanent magnet.

A split test was performed to confirm the heterogeneity of [Dppf@Sil@NMag](RuO₄)₂ **8** using the model reaction. The catalyst was isolated magnetically after the completion of 50% of reaction (determined by gas chromatography, GC). Furthermore, the reaction was allowed to continue for 8 h. Consequently, the reaction failed to proceed which was revealed from GC-MS analysis. In addition, no leaching of the metallic moiety in the reaction mixture was suggested by inductively coupled plasma-optical emission spectroscopy (ICP-OES) analysis. Conclusively, the course of reaction was operated in heterogeneous mode.

By virtue of industrial and green chemistry standpoints, the recycling of the catalyst is very significant in commercial operations. The model reaction was performed with optimized parameters in order to test the reusability of [Dppf@Sil@NMag](RuO₄)₂ **8**. Subsequently, **8** was isolated magnetically, washed with THF, and dried under vacuum after each consecutive run. As illustrated in Fig. 7, the product yield was well maintained between 97–90% from the 1st to 6th run during recycling studies. FT-IR spectroscopy, TEM, and XRD analyses of recycled [Dppf@Sil@NMag](RuO₄)₂ **8** after six consecutive runs was undertaken to confirm its stability. Gratifyingly, similar peak patterns in the FT-IR spectra of both fresh and reused **8** (Fig. 1e, f), suggested retention of functional groups



Scheme 2. Plausible mechanism for the [Dppf@Sil@NMag](RuO₄)₂ **8** promoted oxidation of alcohols.

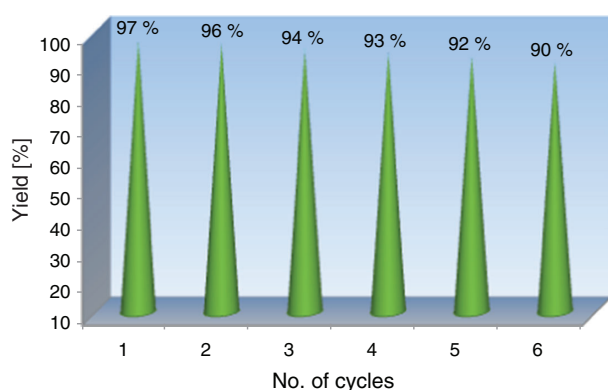


Fig. 7. Reusability of [Dppf@Sil@NMag](RuO₄)₂ **8** in the selective oxidation of benzyl alcohol.

after recycling. TEM images of fresh and reused **8** (Fig. 3a–e) indicated no alteration in morphology even after six consecutive runs. In the X-ray diffractograms of fresh and reused **8** (Fig. 4d–e), diffraction peaks coincide with the cubic inverse spinel structure of the Fe₃O₄ nanocore (JCPDS card no. 86-1339).

Consequently, the stability of **8** was confirmed as no chemical or physical deformations were observed after reusability studies.

Conclusion

In conclusion, we have prepared a new magnetic nanoparticle supported ionic liquid phase catalyst containing perruthenate anions. The catalyst displayed excellent catalytic activity in the selective oxidation of primary alcohols to aldehydes. The catalyst can be expediently isolated and recovered from the reaction mixture with aid of an external magnet and can be reused six times without considerable loss in catalytic activity. The excellent yields, hassle free magnetic retrievability, and recyclability are some prominent features of this protocol.

Experimental

General Remarks

Dried glassware was used to perform all reactions in an air atmosphere. KBr discs of samples (~5% w/w) were used to record FT-IR spectra on a Perkin–Elmer FTIR spectrophotometer. A Bruker-AX8 X-ray diffractometer was employed for XRD analysis. The elemental compositions of samples were investigated by an energy-dispersive X-ray spectrometer, which

was attached to a field emission scanning electron microscope (OXFORD, Instruments). The INCA energy software was employed for ZAF correction of EDX data. ^1H and ^{13}C NMR spectra were recorded on a Bruker AC spectrometer (75 MHz for ^{13}C NMR and 300 MHz for ^1H NMR) using CDCl_3 as solvent and tetramethylsilane (TMS) as an internal standard. The values of chemical shifts δ and coupling constants are expressed in parts per million (ppm) and hertz (Hz) respectively. A Shimadzu QP2010 GCMS was employed to record mass spectra. A transmission electron microscope (JEOL JEM 2100 (200 kV)) was used to investigate the morphology of the materials. A MEL-TEMP capillary melting point apparatus was used to determine melting points and are uncorrected. XPS spectra were recorded on a PHI 5000 Versa Prob II, FEI Inc. X-ray photoelectron spectrometer. Magnetic behaviour of material was scrutinized using a USA, Model 7407 Lake Shore Magnetometer. All other chemicals were used without further purification, which were received from local suppliers.

Preparation of Fe_3O_4 MNPs (NMag 1)

The chemical co-precipitation method was employed to prepare Fe_3O_4 MNPs according to the procedure reported in the literature.^[82] A stock solution was prepared by dissolving $\text{FeCl}_2 \cdot 4\text{H}_2\text{O}$ (2.0 g), $\text{FeCl}_3 \cdot 6\text{H}_2\text{O}$ (5.2 g), and HCl (12 mol L^{-1} , 0.85 mL) in 25 mL of distilled water. A beaker containing aqueous NaOH (1.5 mol L^{-1} , 250 mL) was heated maintaining a temperature of 80°C and the dropwise addition of stock solution was carried out under a nitrogen atmosphere with vigorous stirring. The magnetic separation of Fe_3O_4 MNPs was achieved and they were subsequently washed with distilled water. FT-IR ν_{max} (KBr, thin film)/ cm^{-1} 1690, 1417, 882, 720, 647, 589.

Preparation of Sil@NMag 2

The coating of a silica layer on Fe_3O_4 MNPs was achieved by a sol-gel approach by following the literature procedure.^[83] Fe_3O_4 MNPs 1 (1.0 g) were homogeneously dispersed in a mixture of deionized water (20 mL), ethanol (60 mL), and concentrated aqueous ammonia solution (1.5 mL, 28 wt-%) and ultrasonicated for 0.5 h. Subsequently, dropwise addition of a tetraethylorthosilicate (TEOS) solution (0.45 mL of TEOS in 10 mL of ethanol) was carried out in suspension under vigorous mechanical stirring. The resultant silica coated Fe_3O_4 MNPs 2 were isolated by an external magnetic field, washed three times with ethanol, and dried under vacuum. FT-IR ν_{max} (KBr, thin film)/ cm^{-1} 1222, 1057, 959, 795, 555.

Preparation of 3.Cl.Pr.Sil@NMag 4

The 3-chloropropyl modified Fe_3O_4 MNPs 4 were prepared on the basis of the method reported in the literature.^[84] Fe_3O_4 MNPs coated with silica shell 2 (1 g) were suspended in 50 mL of dry xylene. To the above suspension, 3-chloropropyltriethoxysilane 3 (5 mmol, 1 mL) was added slowly. The reaction mixture was refluxed for 24 h and subsequently cooled to afford the 3-chloropropyl modified Fe_3O_4 MNPs 4. The product was washed three times with deionized water (25 mL), methanol (25 mL), and xylene (25 mL) and dried under vacuum at 50°C . FT-IR ν_{max} (KBr, thin film)/ cm^{-1} 2942, 1890, 1643, 1062, 795.

Preparation of [Dppf@Sil@NMag]Cl 6

Bis(diphenylphosphino)ferrocene 5 (0.731 g, 1 mmol) was added to a suspension of 4 (1 g) in 25 mL of DMF. The reaction mixture was heated at 80°C for 72 h. The insoluble product was

isolated via magnetic separation, washed three times with CH_2Cl_2 (50 mL), DMF (50 mL), and methanol (50 mL), and dried under vacuum to yield [Dppf@Sil@NMag]Cl 6. FT-IR ν_{max} (KBr, thin film)/ cm^{-1} 3314, 1691, 1549, 1437, 1341, 1059, 961, 692, 466. Anal. Calc. for 0.2 mmol of Dppf units g^{-1} of 6: Found: C 33.59, O 51.53, Cl 0.57, Fe 4.56, P 0.60, Si 9.15 %.

Preparation of [Dppf@Sil@NMag](RuO₄)₂ 8

Potassium perruthenate 7 (0.4 mmol, 0.211 g) was added to a suspension of 6 (1 g) in distilled water (20 mL). The mixture was stirred for 24 h. Afterwards, the isolation of insoluble product was achieved using an external bar magnet. Washing with distilled water furnished [Dppf@Sil@NMag](RuO₄)₂ 8. FT-IR ν_{max} (KBr, thin film)/ cm^{-1} 3393, 2937, 1636, 1439, 1063, 887, 865, 569, 470. Anal. Calc. for 0.11 mmol Ru g^{-1} of 8: Found: C 36.10, O 43.74, Fe 9.24, P 0.53, Ru 1.2, Si 9.19 %.

General Procedure for Oxidation of Alcohol

A primary alcohol (1 mmol) was added to a suspension of 50 mg of [Dppf@Sil@NMag](RuO₄)₂ 8 in 5 mL of THF and refluxed. TLC was used to monitor the reaction progress. Compound 8 was isolated magnetically after completion of the reaction. Column chromatography (ethyl acetate/petroleum ether) was used to purify the reaction mixture to afford pure products.

Supplementary Material

Spectroscopic data of the synthesized aldehydes are available on the Journal's website.

Conflicts of Interest

The authors declare no conflicts of interest.

Acknowledgements

This work was financially supported by the Science and Engineering Research Board (SERB), New Delhi, under Start-Up Research Grant (Young Scientists) – Chemical Sciences (NO. SB/FT/CS-060/2014).

References

- [1] H. C. Erythropel, J. B. Zimmerman, T. M. de Winter, L. Petitjean, F. Melnikov, C. H. Lam, A. W. Lounsbury, K. E. Mellor, N. Z. Janković, Q. Tu, L. N. Pincus, M. M. Falinski, W. Shi, P. Coish, D. L. Plata, P. T. Anastas, *Green Chem.* **2018**, *20*, 1929. doi:10.1039/C8GC00482J
- [2] P. T. Anastas, J. C. Warner, *Green Chemistry: Theory and Practice* **1998** (Oxford University Press: New York, NY).
- [3] C. Van Doorslaer, J. Wahlen, P. Mertens, K. Binnemans, D. De Vos, *Dalton Trans.* **2010**, *39*, 8377. doi:10.1039/C001285H
- [4] V. Campisciano, F. Giacalone, M. Gruttadauria, *Chem. Rec.* **2017**, *17*, 918. doi:10.1002/TCR.201700005
- [5] F. Giacalone, M. Gruttadauria, *ChemCatChem* **2016**, *8*, 664. doi:10.1002/CCTC.201501086
- [6] X. Zheng, S. Luo, L. Zhang, J.-P. Cheng, *Green Chem.* **2009**, *11*, 455. doi:10.1039/B823123K
- [7] A. Riisager, R. Fehrmann, M. Haumann, P. Wasserscheid, *Eur. J. Inorg. Chem.* **2006**, 695. doi:10.1002/EJIC.200500872
- [8] G. Molteni, A. M. Ferretti, S. Mondini, A. Ponti, *J. Nanopart. Res.* **2018**, *20*, 79. doi:10.1007/S11051-018-4184-8
- [9] S. Shylesh, V. Schünemann, W. R. Thiel, *Angew. Chem. Int. Ed.* **2010**, *49*, 3428. doi:10.1002/ANIE.200905684
- [10] H.-Y. Lü, S.-H. Yang, J. Deng, Z.-H. Zhang, *Aust. J. Chem.* **2010**, *63*, 1290. doi:10.1071/CH09532
- [11] H. Dadhania, D. Raval, A. Dadhania, *Polycyclic Aromat. Compd.* **2019**, doi:10.1080/10406638.2019.1595057
- [12] J. S. Ghomi, S. Zahedi, *Ultrason. Sonochem.* **2017**, *34*, 916. doi:10.1016/J.ULTSONCH.2016.08.003

- [13] H. T. Nguyen, N.-P. T. Le, D.-K. N. Chau, P. H. Tran, *RSC Adv.* **2018**, *8*, 35681. doi:10.1039/C8RA04893B
- [14] R.-Q. Yang, N. Zhang, X.-G. Meng, X.-H. Liao, L. Li, H.-J. Song, *Aust. J. Chem.* **2018**, *71*, 559. doi:10.1071/CH18138
- [15] A. L. Cappelletti, P. M. Uberman, S. E. Martín, M. E. Saleta, H. E. Troiani, R. D. Sánchez, R. E. Carbonio, M. C. Strumia, *Aust. J. Chem.* **2015**, *68*, 1492. doi:10.1071/CH14722
- [16] H.-Y. Lü, S.-H. Yang, J. Deng, Z.-H. Zhang, *Aust. J. Chem.* **2010**, *63*, 1290. doi:10.1071/CH09532
- [17] Y.-R. Cui, C. Hong, Y.-L. Zhou, Y. Li, X.-M. Gao, X.-X. Zhang, *Talanta* **2011**, *85*, 1246. doi:10.1016/J.TALANTA.2011.05.010
- [18] P. B. Shete, R. M. Patil, B. M. Tiwale, S. H. Pawar, *J. Magn. Magn. Mater.* **2015**, *377*, 406. doi:10.1016/J.JMMM.2014.10.137
- [19] S. Kumari, R. P. Singh, *Int. J. Biol. Macromol.* **2012**, *51*, 76. doi:10.1016/J.IJBIOMAC.2012.01.040
- [20] J. Mao, W. Jiang, J. Gu, S. Zhou, Y. Lu, T. Xie, *Appl. Surf. Sci.* **2014**, *317*, 787. doi:10.1016/J.APSUSC.2014.08.191
- [21] M. H. Mashhadizadeh, M. Amoli-Diva, M. R. Shapouri, H. Afruzi, *Food Chem.* **2014**, *151*, 300. doi:10.1016/J.FOODCHEM.2013.11.082
- [22] S. Rengshausen, F. Etscheidt, J. Großkurth, K. L. Luska, A. Bordet, W. Leitner, *Synlett* **2019**, *30*, 405. doi:10.1055/S-0037-1611678
- [23] L. Offner-Marko, A. Bordet, G. Moos, S. Tricard, S. Rengshausen, B. Chaudret, K. L. Luska, W. Leitner, *Angew. Chem. Int. Ed.* **2018**, *57*, 12721. doi:10.1002/ANIE.201806638
- [24] M. Nasrollahzadeh, Z. Issaabadi, S. Mohammad Sajadi, *RSC Adv.* **2018**, *8*, 27631. doi:10.1039/C8RA04368J
- [25] C. Garkoti, J. Shabir, S. Mozumdar, *New J. Chem.* **2017**, *41*, 9291. doi:10.1039/C6NJ03985E
- [26] R. Teimuri-Mofrad, S. Esmati, M. Rabiei, M. Gholamhosseini-Nazari, *Heterocycl. Commun.* **2017**, *23*, 439. doi:10.1515/HC-2017-0140
- [27] S.-Q. Bai, L. Jiang, S.-L. Huang, M. Lin, S.-Y. Zhang, M.-Y. Han, J. Xu, Y. Lu, G.-X. Jin, T. S. Andy Hor, *Aust. J. Chem.* **2014**, *67*, 1387. doi:10.1071/CH14148
- [28] M. B. Gawande, P. S. Branco, R. S. Varma, *Chem. Soc. Rev.* **2013**, *42*, 3371. doi:10.1039/C3CS35480F
- [29] Z. Zarnegar, J. Safari, *J. Nanopart. Res.* **2014**, *16*, 2509. doi:10.1007/S11051-014-2509-9
- [30] Y. Qiao, H. Li, L. Hua, L. Orzechowski, K. Yan, B. Feng, Z. Pan, N. Theysen, W. Leitner, Z. Hou, *ChemPlusChem* **2012**, *77*, 1128. doi:10.1002/CPLU.201200246
- [31] D. I. Enache, J. K. Edwards, P. Landon, B. Solsona-Espriu, A. F. Carley, A. A. Herzing, M. Watanabe, C. J. Kiely, D. W. Knight, G. J. Hutchings, *Science* **2006**, *311*, 362. doi:10.1126/SCIENCE.1120560
- [32] M. Beller, C. Bolm, *Transition Metals for Organic Synthesis*, 2nd edn **2004** (Wiley-VCH Verlag GmbH & Co. KGaA: Weinheim).
- [33] T. J. Zerk, P. W. Moore, J. S. Harbort, S. Chow, L. Byrne, G. A. Koutsantonis, J. R. Harmer, M. Martínez, C. M. Williams, P. V. Bernhardt, *Chem. Sci.* **2017**, *8*, 8435. doi:10.1039/C7SC04260D
- [34] P. W. Moore, C. D. G. Read, P. V. Bernhardt, C. M. Williams, *Chem. – Eur. J.* **2018**, *24*, 4556. doi:10.1002/CHEM.201800531
- [35] B. Karimi, D. Elhamifar, O. Yari, M. Khorasani, H. Vali, J. H. Clark, A. J. Hunt, *Chem. – Eur. J.* **2012**, *18*, 13520. doi:10.1002/CHEM.201200380
- [36] R. Ciriminna, P. Hesemann, J. J. E. Moreau, M. Carraro, S. Campestrini, M. Pagliaro, *Chem. – Eur. J.* **2006**, *12*, 5220. doi:10.1002/CHEM.200501556
- [37] Y. Xie, Z. Zhang, S. Hu, J. Song, W. Li, B. Han, *Green Chem.* **2008**, *10*, 278. doi:10.1039/B715067A
- [38] J. Lybaert, B. U. W. Maes, K. Abbaspour Tehrani, K. De Wael, *Electrochim. Acta* **2015**, *182*, 693. doi:10.1016/J.ELECTACTA.2015.09.107
- [39] N. Ghalavand, M. M. Heravi, M. R. Nabid, R. Sedghi, *J. Alloys Compd.* **2019**, *799*, 279. doi:10.1016/J.JALLCOM.2019.05.209
- [40] M. Mohammadi, A. Khazaei, A. Rezaei, Z. Huajun, S. Xuwei, *ACS Sustain. Chem. & Eng.* **2019**, *7*, 5283. doi:10.1021/ACS.SUSCHEMENG.8B06279
- [41] V. Panwar, P. Kumar, S. S. Ray, S. L. Jain, *Tetrahedron Lett.* **2015**, *56*, 3948. doi:10.1016/J.TETLET.2015.05.003
- [42] T. M. A. Shaikh, L. Emmanuvel, A. Sudalai, *J. Org. Chem.* **2006**, *71*, 5043. doi:10.1021/JO0606305
- [43] M. Uyanik, K. Ishihara, *Chem. Commun.* **2009**, 2086. doi:10.1039/B823399C
- [44] Y. Sun, H. Ma, Y. Luo, S. Zhang, J. Gao, J. Xu, *Chem. – Eur. J.* **2018**, *24*, 4653. doi:10.1002/CHEM.201705824
- [45] F. Mao, Z. Qi, H. Fan, D. Sui, R. Chen, J. Huang, *RSC Adv.* **2017**, *7*, 1498. doi:10.1039/C6RA27073E
- [46] M. A. Nasser, K. Hemmat, A. Allahresani, E. Hamidi-Hajiabadi, *Appl. Organomet. Chem.* **2019**, *33*, e4809. doi:10.1002/AOC.4809
- [47] J. M. Hoover, J. E. Steves, S. S. Stahl, *Nat. Protoc.* **2012**, *7*, 1161. doi:10.1038/NPROT.2012.057
- [48] X. Yan, X. Yue, K. Liu, Z. Hao, Z. Han, J. Lin, *Front Chem.* **2019**, *7*, 394. doi:10.3389/FCHEM.2019.00394
- [49] R. Ray, S. Chandra, D. Maiti, G. K. Lahiri, *Chem. – Eur. J.* **2016**, *22*, 8814. doi:10.1002/CHEM.201601800
- [50] X.-T. Zhou, H.-B. Ji, S.-G. Liu, *Tetrahedron Lett.* **2013**, *54*, 3882. doi:10.1016/J.TETLET.2013.05.055
- [51] H. A. Beejapur, F. Giacalone, R. Noto, P. Franchi, M. Lucarini, M. Gruttadauria, *ChemCatChem* **2013**, *5*, 2991. doi:10.1002/CCTC.201300234
- [52] H. A. Beejapur, V. Campisciano, F. Giacalone, M. Gruttadauria, *Adv. Synth. Catal.* **2015**, *357*, 51. doi:10.1002/ADSC.201400641
- [53] J. Fan, F. Pu, M. Sun, Z.-W. Liu, X.-Y. Han, J.-F. Wei, X.-Y. Shi, *New J. Chem.* **2016**, *40*, 10498. doi:10.1039/C6NJ01476C
- [54] F. Shi, M. K. Tse, M. Beller, *Chem. Asian J.* **2007**, *2*, 411. doi:10.1002/ASIA.200600383
- [55] A. V. Biradar, M. K. Dongare, S. B. Umbarkar, *Tetrahedron Lett.* **2009**, *50*, 2885. doi:10.1016/J.TETLET.2009.03.178
- [56] R. Kurane, J. Jadhav, S. Khanapure, R. Salunkhe, G. Rashinkar, *Green Chem.* **2013**, *15*, 1849. doi:10.1039/C3GC40592C
- [57] A. Naikwade, M. Jagadale, D. Kale, S. Gajare, G. Rashinkar, *Catal. Lett.* **2018**, *148*, 3178. doi:10.1007/S10562-018-2514-1
- [58] S. Khanapure, M. Jagadale, D. Kale, S. Gajare, G. Rashinkar, *Aust. J. Chem.* **2019**, *72*, 513. doi:10.1071/CH18576
- [59] M. Kooti, M. Afshari, *Mater. Res. Bull.* **2012**, *47*, 3473. doi:10.1016/J.MATERRESBULL.2012.07.001
- [60] M. A. Zolfigol, R. Ayazi-Nasrabadi, *RSC Adv.* **2016**, *6*, 69595. doi:10.1039/C6RA11620E
- [61] C. Tang, Z. Zou, Y. Fu, K. Song, *ChemistrySelect* **2018**, *3*, 5987. doi:10.1002/SLCT.201800610
- [62] H. B. Friedrich, N. Singh, *Catal. Lett.* **2006**, *110*, 61. doi:10.1007/S10562-006-0099-6
- [63] Q. Dong, X. Zhuang, Z. Li, B. Li, B. Fang, C. Yang, H. Xie, F. Zhang, X. Feng, *J. Mater. Chem. A* **2015**, *3*, 7767. doi:10.1039/C5TA00556F
- [64] M. K. Kolel-Veetil, R. M. Gamache, N. Bernstein, R. Goswami, S. B. Qadri, K. P. Fears, J. B. Miller, E. R. Glaser, T. M. Keller, *J. Mater. Chem. C* **2015**, *3*, 11705. doi:10.1039/C5TC02956B
- [65] C. M. Woodbridge, D. L. Pugmire, R. C. Johnson, N. M. Boag, M. A. Langell, *J. Phys. Chem. B* **2000**, *104*, 3085. doi:10.1021/JP993235+
- [66] F. Rondino, D. Catone, G. Mattioli, A. A. Bonapasta, P. Bolognesi, A. R. Casavola, M. Coreno, P. O'Keeffe, L. Avaldi, *RSC Adv.* **2014**, *4*, 5272. doi:10.1039/C3RA45705B
- [67] R. K. Blundell, P. Licence, *Phys. Chem. Chem. Phys.* **2014**, *16*, 15278. doi:10.1039/C4CP01901F
- [68] Y. Nonoguchi, Y. Iihara, K. Ohashi, T. Murayama, T. Kawai, *Chem. Asian J.* **2016**, *11*, 2423. doi:10.1002/ASIA.201600810
- [69] L. Ji, L. Zhou, X. Bai, Y. Shao, G. Zhao, Y. Qu, C. Wang, Y. Li, *J. Mater. Chem.* **2012**, *22*, 15853. doi:10.1039/C2JM32896H
- [70] S. Ghosh, A. Z. M. Badruddoza, M. S. Uddin, K. Hidajat, *J. Colloid Interface Sci.* **2011**, *354*, 483. doi:10.1016/J.JCIS.2010.11.060
- [71] S. Kanemoto, S. Matsubara, K. Takai, K. Oshima, K. Utimato, H. Nozaki, *Bull. Chem. Soc. Jpn* **1988**, *61*, 3607. doi:10.1002/AOC.3510

- [74] K. B. Sharpless, K. Akashi, K. Oshima, *Tetrahedron Lett.* **1976**, *17*, 2503.
- [75] D. G. Lee, L. N. Congson, *Can. J. Chem.* **1990**, *68*, 1774. doi:10.1002/AOC.3477
- [76] U. Siemeling, T.-C. Auch, *Chem. Soc. Rev.* **2005**, *34*, 584. doi:10.1039/B315486F
- [77] R. C. J. Atkinson, V. C. Gibson, N. J. Long, *Chem. Soc. Rev.* **2004**, *33*, 313. doi:10.1039/B316819K
- [78] *Ferrocenes: Homogeneous Catalysis, Organic Synthesis, Material Science* (Eds A. Togni, T. Hayashi) **1995** (Wiley-VCH: Weinheim).
- [79] T. J. Colacot, *Platin. Met. Rev.* **2001**, *45*, 22.
- [80] P. Barbaro, C. Bianchini, G. Giambastiani, S. L. Parisel, *Coord. Chem. Rev.* **2004**, *248*, 2131. doi:10.1016/J.CCR.2004.03.022
- [81] *Metallocenes* (Eds A. Togni, R. L. Halterman) **1998** (Wiley-VCH: Weinheim).
- [82] X. Zhao, Y. Shi, T. Wang, Y. Cai, G. Jiang, *J. Chromatogr. A* **2008**, *1188*, 140. doi:10.1016/J.CHROMA.2008.02.069
- [83] D. Yang, J. Hu, S. Fu, *J. Phys. Chem. C* **2009**, *113*, 7646. doi:10.1021/JP900868D
- [84] A. Naikwade, M. Jagadale, D. Kale, S. Gajare, P. Bansode, G. Rashinkar, *Appl. Organometal. Chem.* **2019**, *33*, e5066